

Generation of valley polarized current in bilayer graphene

D. S. L. Abergel^{a)} and Tapash Chakraborty

Department of Physics and Astronomy, University of Manitoba, Winnipeg R3T 2N2, Canada

(Received 17 June 2009; accepted 25 July 2009; published online 14 August 2009)

We propose a device for the generation of valley polarized electronic current in bilayer graphene. By analyzing the response of this material to intense terahertz frequency light in the presence of a transverse electric field, we demonstrate that dynamical states are induced in the gapped energy region, and if the system parameters are properly tuned, these states exist only in one valley. The valley polarized states can then be used to filter an arbitrary electron current, so generating a valley polarized current. © 2009 American Institute of Physics. [DOI: 10.1063/1.3205117]

One particularly interesting feature of mono- and bilayer graphene^{1–3} is the valley degree of freedom. The six corners of the Brillouin zone (the K points in the inset to Fig. 1) are separated from each other in momentum space, and the geometry of the reciprocal lattice requires that opposite corners are inequivalent so that there are two species of K point, called “valleys.”⁴ The low energy spectrum is localized near the six K points, so that in this limit, which of the two valleys the electron momentum is located in becomes a good quantum number. The valley degree of freedom therefore constitutes a two state system (analogous to the electron spin) and is often called the “isospin.” This has prompted the suggestion that the isospin could be manipulated and controlled in a useful way (so-called “valleytronics”), for example, to make a solid state qubit.⁵ Of course, in order to achieve this goal, one must be able to accurately prepare and manipulate electron states in one valley or another, and to date there have been several proposals for devices which purport to achieve this.^{5–10} Recently, attention has also turned to the optical properties of monolayer graphene, and its response to linearly and circularly polarized irradiating light fields has shown interesting features resulting from the chirality of the electrons and the linear low energy spectrum.^{11,12}

In this letter, we combine these areas of interest and analyze the response of the energy spectrum of gapped bilayer graphene^{2,13} to external electromagnetic radiation in the terahertz frequency range. We then propose a device which filters electrons according to which valley they are in, creating a valley polarized current. Specifically, we find that the different sublattice composition of the wave functions of electrons in opposite valleys causes them to interact with the irradiating field asymmetrically. When the radiation and system parameters are properly tuned, dynamical states existing entirely in one valley are induced. If a current of electrons in this energy range is passed through the irradiated region, the absence of available states in one valley means that those electrons are unable to pass, while electrons in the other valley may. The current exiting the irradiated region is therefore comprised of electrons in only one valley, a so-called “valley polarized current.”

This filtering effect is a direct result of the valley asymmetric density of states in the irradiated region, and is therefore a bulk effect, independent of the geometry of the sample

and its edges. This gives our device a significant advantage over many prior proposals as it does not rely on the precise construction of an edge (as in Refs. 5–7), or the exact deposition of a gate along one crystallographic direction (as in Ref. 8), both of which are very challenging tasks. Reference 10 also necessitates a complex gating arrangement to support one-dimensional channels in the graphene. Even if these devices could be manufactured, the currents they produce are often only partially polarized, and are localized in one-dimensional channels, whereas our proposal shows complete valley polarization for significant current flow in a bulk situation, making the potential for applications of the current generated by this device much more plausible.

We model irradiated bilayer graphene using the Hamiltonian $\mathcal{H}=H_0+H_U+H(t)$, where H_0 is the Hamiltonian of ungated, unirradiated graphene, and H_U represents the inter-layer potential difference generated by the top gate.⁴ The time dependent term $H(t)$ is the Hamiltonian of the irradiating field, described by making the Peierls substitution in H_0+H_U with the vector potential $\mathbf{A}=F/|\Omega|[\cos \Omega t, \sin \Omega t]$ (where Ω is the frequency of the radiation) giving

$$H(t) = \frac{\xi v_F e F}{|\Omega|} \begin{pmatrix} 0 & 1 \\ 1 & 0 \end{pmatrix} \otimes \begin{pmatrix} 0 & e^{-i\Omega t} \\ e^{i\Omega t} & 0 \end{pmatrix}.$$

The opposite orientation of the circular polarization is employed by substituting $\Omega \rightarrow -\Omega$ in this definition. The natural parameter by which to measure the strength of coupling of the electrons to the field is $x=(v_F e F)/(\hbar \Omega^2)$, where F is the field intensity, Ω is the frequency of the radiation, and v_F is the Fermi velocity. If $x > 1$ we say we are in the strongly irradiated regime. We take the dipole approximation and assume that the graphene is clean enough that we can ignore intervalley scattering caused by defects such as lattice imperfections. We also neglect electron-electron interactions. The time dependent part of the Hamiltonian is periodic with period $T_0=2\pi/\Omega$, so we can employ Floquet’s theorem¹⁴ to write the electron wave functions $\Psi(t)$ in the irradiated region as $\Psi_A(t)=e^{-i\varepsilon_A t}\Phi_A(t)$ where the coefficient ε_A is the energy of the dynamical state (called the “quasienergy”). The wave function in the temporal Brillouin zone $\Phi_A(t)$, defined for $-\pi/\Omega < t < \pi/\Omega$, is periodic in time and can be expanded over its Fourier components n and the state basis consisting of eigenfunctions of the static Hamiltonian denoted ψ_α . We therefore write

^{a)}Electronic mail: abergel@cc.umanitoba.ca.

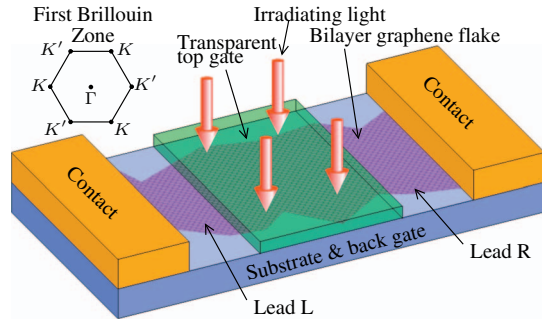


FIG. 1. (Color) Schematic of the valley filtering device. The area under the transparent top gate is irradiated, and the parts of the flake lying outside of the gated region function as the graphitic leads. The inset shows the first Brillouin zone.

$$\Psi_A(\mathbf{x}, t) = \sum_{n=-\infty}^{\infty} \sum_{\alpha} e^{in\Omega t} \chi_{n\alpha}^A \psi_{\alpha}(\mathbf{x}). \quad (1)$$

We solve the time dependent Schrödinger equation for \mathcal{H} by taking the Fourier transform of the matrix elements of the Hamiltonian over the states ψ_{α} and constructing the Floquet matrix.¹⁴ Diagonalizing this matrix yields the quasienergies and the wave function coefficients $\chi_{n\alpha}^A$.

In Fig. 2 we show the low energy spectrum of irradiated bilayer graphene with and without a static gap in each of the two valleys. The color of the line indicates the weight of the static component of the wave function, which represents the physically observable part of the dynamical state. In the left-hand column, the coupling parameter is $x=0.96$ (weakly irradiated) while in the right-hand column $x=4.82$ (strongly irradiated). We superimpose the unirradiated ($F=0$) spectrum (red lines) for comparison. The radiation opens dynamical gaps at $\hbar\Omega/2$ intervals (as was shown in the monolayer case¹¹). Second, when there is a gate potential applied, dynamical states are present in the gapped region (see the lower two rows), and the quadratic shape of the low momentum part of the bands is restored for strong radiation. However, because K electrons couple more strongly to the radiation than K' electrons (due to the different sublattice composition of the wave functions), the weights of the static component of the Floquet states are drastically different in each valley. In the strongly irradiated regime, the notion of the static gap loses its meaning as there are many dynamical states with significant static component in that energy range. It is the dynamical states in the static gap which we utilize in the proposal for the valley filtering device. Reversing the polarization of the light or the orientation of U causes the K' valley to couple strongly.

We now demonstrate the generation of valley polarized current by using irradiated bilayer graphene as a filter for an arbitrary current. We employ a tunneling approach¹⁵ where we suppose that the system consists of three parts, as shown in Fig. 1. They are the two graphitic “leads” described by Hamiltonians H_L , $H_R=H_0$ with energy spectrum E_{α} and chemical potential $\pm\mu/2$, and the central, irradiated region described by the time dependent Hamiltonian $H_C=\mathcal{H}$ discussed above, with quasienergy spectrum ε_A and chemical potential fixed at zero. The contacts shown in Fig. 1 connect the graphene flake with external systems, and we do not consider their influence. The central region is linked to the leads via the coupling Hamiltonians H_{CL} , H_{CR} . Denoting the

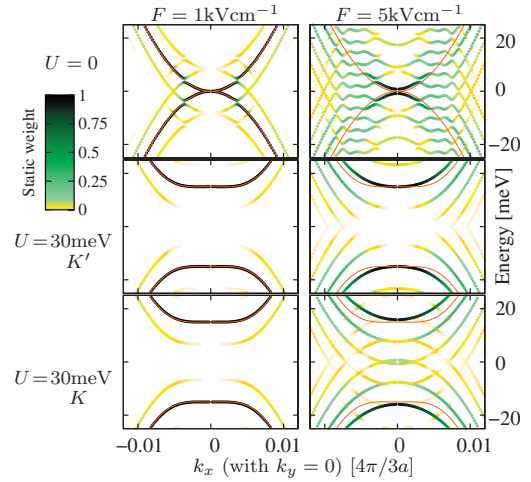


FIG. 2. (Color) The quasienergy spectrum for $U=0$ (top line) and $U=30$ meV (lower two lines) in both valleys, for weak radiation (left) and strong radiation (right). The color of the line indicates the weight of the static ($n=0$) component. Thin red lines show the unirradiated spectrum.

operators for electrons in the leads by c_{kai} for $i \in \{L, R\}$, and the central area by d_{qA} , we have

$$H_{Ci} = \sum_{\mathbf{k}, \alpha, q, A} V_{\mathbf{k}\alpha, qA} c_{kai}^{\dagger} d_{qA} + \text{H.C.}$$

We assume that the central region is wide enough to forbid electrons from tunneling directly between the two leads. Since it has been shown¹⁶ that transmission from bilayer graphene into gapped bilayer graphene is high for a wide range of the electron’s angle of momentum, we assume that for the transfer to occur, the electron’s momentum is conserved and the energy of the states in the two regions must be sufficiently close. We parameterize this closeness by writing the function $\Delta(E)$ such that $\Delta(E)=0$ for $|E|>\eta$ and $\Delta(0)=1$ so that η describes the width of the allowed transition. Then, the coupling parameter is $V_{\mathbf{k}\alpha, qA} = \mathcal{V} \delta_{\mathbf{k}, q} \Delta(E_{\mathbf{k}\alpha} - \varepsilon_{qA}) |\chi_{0\alpha}^A|^2$. The quantity \mathcal{V} has units of energy and parameterizes the maximal strength of the coupling and we preserve the electron momentum via the δ function.

The valley component of the charge current in the right-hand lead is $J_{\xi} = -\langle dN_R^{\xi}/dt \rangle$, where N_R^{ξ} is the number operator

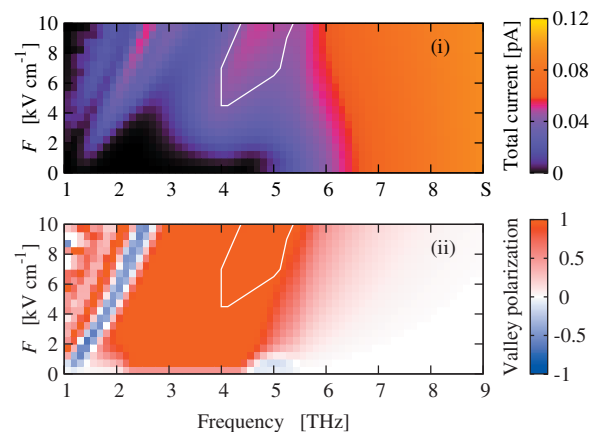


FIG. 3. (Color) (i) The total current and (ii) the valley polarization as a function of the field parameters. In both plots, $U=20$ meV, $\mu=12$ meV, and $\eta=0.3 \times \hbar\Omega$ with $\Omega=2$ THz. The white contours denote the region of high valley polarization and significant current flow.

for the appropriate electron species. Using a nonequilibrium Green's function analysis and taking the steady state limit, we find that the current is

$$J_{\xi} = -\frac{2e}{\hbar} \int \frac{d^2\mathbf{k}}{(2\pi)^2} \sum_{\alpha_{\xi}} \text{Tr}\{\bar{\Gamma}_{\alpha_{\xi}} \mathcal{J} \bar{G}^r(E_{\alpha_{\xi}})\} \mathcal{F}, \quad (2)$$

where $\mathcal{J} \bar{G}^r$ is the imaginary part of the full retarded Green's function in the central region, $\bar{\Gamma}$ contains the coupling parameters, and $\mathcal{F} = f_c(E_{\alpha_{\xi}}) - f_R(E_{\alpha_{\xi}})$ depends on the distribution functions in the right lead and central region. The central region Green's function is calculated using the Floquet states derived above, and includes the self energy due to the two leads.

To characterize the degree of valley polarization of the current, we define $\mathcal{P} = (J_K - J_{K'}) / (J_K + J_{K'})$ so that $\mathcal{P} = -1(+1)$ corresponds to fully $K'(K)$ polarized current. In Fig. 3 we plot the total current and the polarization as a function of the radiation intensity and frequency for $U = 20$ meV and the chemical potentials of the leads arranged to drive current in the energy range corresponding to the static gap ($\mu = 12$ meV). The area enclosed by the white contour shows where $J > 0.04$ pA and $\mathcal{P} > 0.98$ simultaneously, i.e., the region where the system parameters are tuned for significant current *and* very high polarization. Reversing the sign of U or the orientation of the polarization of the radiation leaves Fig. 3(i) unchanged, but inverts Fig. 3(ii) so that the region of high current and polarization is in the K' valley. Identification of the valley into which the current is polarized may be achieved by application of an in-plane electric field⁷ which produces a valley-dependent Hall current which will result in a measurable asymmetry in the electron density across the conducting channel.

In summary, we have described the measurable characteristics of a graphene-based valley polarized current generator, where we expect current of ~ 0.1 pA and valley polarization of $>99\%$. Our work should provide necessary stimulus in the quest for valleytronics with graphene.

D.S.L.A. thanks H. Schomerus for helpful discussions, and this work was supported by the Canada Research Chairs program, and the NSERC Discovery Grant.

- ¹K. S. Novoselov, A. K. Geim, S. V. Morozov, D. Jiang, Y. Zhang, S. V. Dubonos, I. V. Grigorieva, and A. A. Firsov, *Science* **306**, 666 (2004); K. S. Novoselov, E. McCann, S. V. Morozov, V. I. Fal'ko, M. I. Katsnelson, U. Zeitler, D. Jiang, F. Schedin, and A. K. Geim, *Nat. Phys.* **2**, 177 (2006).
- ²T. Ohta, A. Bostwick, T. Seyller, K. Horn, and E. Rotenberg, *Science* **313**, 951 (2006).
- ³K. S. Novoselov, A. K. Geim, S. V. Morozov, D. Jiang, M. I. Katsnelson, I. V. Grigorieva, S. V. Dubonos, and A. A. Firsov, *Nature (London)* **438**, 197 (2005); Y. Zhang, Y.-W. Tan, H. Stormer, and P. Kim, *ibid.* **438**, 201 (2005).
- ⁴E. McCann, D. S. L. Abergel, and V. I. Fal'ko, *Eur. Phys. J. Spec. Top.* **148**, 91 (2007).
- ⁵A. Rycerz, J. Tworzydło, and C. W. J. Beenakker, *Nat. Phys.* **3**, 172 (2007); A. R. Akhmerov, J. H. Bardarson, A. Rycerz, and C. W. J. Beenakker, *Phys. Rev. B* **77**, 205416 (2008).
- ⁶G. Tkachov, *Phys. Rev. B* **79**, 045429 (2009); A. Cresti, G. Grosso, and G. P. Parravicini, *ibid.* **77**, 233402 (2008).
- ⁷D. Xiao, W. Yao, and Q. Niu, *Phys. Rev. Lett.* **99**, 236809 (2007).
- ⁸J. M. Pereira, Jr., F. M. Peeters, R. N. Costa Filho, and G. A. Farias, *J. Phys.: Condens. Matter* **21**, 045301 (2009).
- ⁹J. L. Garcia-Pomar, A. Cortijo, and M. Nieto-Vesperinas, *Phys. Rev. Lett.* **100**, 236801 (2008).
- ¹⁰I. Martin, Ya. M. Blanter, and A. F. Morpurgo, *Phys. Rev. Lett.* **100**, 036804 (2008).
- ¹¹S. V. Syzranov, M. V. Fistul, and K. B. Efetov, *Phys. Rev. B* **78**, 045407 (2008); T. Oka, and H. Aoki, *ibid.* **79**, 081406(R) (2009).
- ¹²W. Yao, D. Xiao, and Q. Niu, *Phys. Rev. B* **77**, 235406 (2008); F. J. López-Rodríguez and G. G. Naumis, *ibid.* **78**, 201406(R) (2008).
- ¹³J. B. Oostinga, H. B. Heersche, X. Liu, A. F. Morpurgo, and L. M. K. Vandersypen, *Nature Mater.* **7**, 151 (2008); E. McCann, *Phys. Rev. B* **74**, 161403(R) (2006); E. V. Castro, K. S. Novoselov, S. V. Morozov, N. M. R. Peres, J. M. B. Lopes dos Santos, J. Nilsson, F. Guinea, A. K. Geim, and A. H. Castro Neto, *Phys. Rev. Lett.* **99**, 216802 (2007).
- ¹⁴T. Dittrich, P. Hänggi, G.-L. Ingold, B. Kramer, G. Schön, and W. Zwerger, *Quantum Transport and Dissipation* (Wiley, Weinheim, 1998), Chap. 5.
- ¹⁵H. Haug and A.-P. Jauho, *Quantum Kinetics in Transport and Optics of Semiconductors* (Springer, Berlin, 1998), Chap. 12.
- ¹⁶J. Nilsson, A. H. Castro Neto, F. Guinea, and N. M. R. Peres, *Phys. Rev. B* **76**, 165416 (2007).